Proceedings of Science and Mathematics
Faculty of Science, Universiti Teknologi Malaysia
Vol. 23, 2024, page 30-38

Magnetic Field and Heat Generation Effects on Mixed Convection Heat Transfer in a Lid-Driven Square Cavity

Putri Elia Elyana Shahrin, Mohd Ariff Admon
Department of Mathematical Sciences, Faculty of Science, Universiti Teknologi Malaysia
Corresponding author: ariffadmon@utm.my

Abstract
The study of heat transfer and fluid flow in enclosures has become essential for optimising a variety of industrial processes in recent years. This research focuses on analyze numerically the fluid flow and heat transfer in a lid-driven square cavity with the presence of magnetic field and heat generation. The top and bottom wall are maintained at constant temperatures. Meanwhile, the vertical walls are insulated. The top wall is moving at a constant speed horizontally. The governing partial differential equations are transformed into a non-dimensional form using similarity transformations, and then the finite element method in COMSOL MultiPhysics is used to solve the model numerically. The effects of the parameters on the velocity profile and temperature distribution are examined. Validation of the results is performed by comparing the maximum and minimum value of the horizontal and vertical velocities at the mid-section of the cavity and show minor different between the numbers due to variation of software versions. The influence of Hartmann number, Ha and internal heat generation or absorption, Δ (ranges from 0 to 60 and -5 to 5, respectively) on the thermal characteristics and fluid flow are analyzed. The isotherm and simulated streamlines are displayed. The fluid flow structure and temperature field are shown to be significantly impacted by the Ha. The rate at which heat is transferred reduces as Ha rises because convectional flow is inhibited. Thermal boundary layers close to heat sources reduce in the absence of Δ. On the other hand, Δ strengthens these layers along the colder regions, improving the transfer of heat and minimising temperature differentials close to the heat sources. Although the stream function values rise in the presence of internal heat, the overall fluid flow pattern is essentially unaffected by these changes.
Keywords Magnetic field; Heat generation/absorption; Mixed convection; Square cavity; COMSOL Multiphysics.

1. Introduction

In the world of heat transfer, understanding how heat moves in limited places is important for making things work better, such as in electronics or other engineering systems. Examples of these applications include solar collectors, heat exchanger improvement for thermal performance, and oil extraction in grooved wet clutches [1]. A cavity with a driven lid is used to analyse the properties of heat and fluid movement in the connected challenges. A moving wall or walls can drive the flow, and a temperature gradient between the hot and cool barriers allows heat to travel. In engineering applications, lid-driven cavity geometry is found in a variety of configurations and geometries, such as square, rectangle, triangular, and trapezoidal, among other forms, under a broad range of temperature boundary settings.

Many researchers have studied the end wall effects of lid-driven cavity flows [2, 3]. Benchmark results for two-dimensional lid-driven square cavity flow at high Reynold numbers using a multigrid technique have been produced, [4]. Their study established an example for numerical precision and has been often cited in other studies.Later studies have investigated the effects of aspect ratios on cavity flow and vortex behaviour across a broad range of Reynolds numbers using a variety of numerical techniques, such as the lattice Boltzmann technique and finite difference methods [5, 6, 7].

Numerical simulations have been widely used in the study of these phenomena because they offer an inexpensive way to illuminate heat transport pathways. Mixed convection, which combines forced and free convection flows, is crucial in many technical and industrial applications, such as thermal insulation and geothermal reservoirs [8]. For example, research on mixed convection in square cavities by [9] and [10] has provided insights into heat transfer rates and fluid flow behaviour that are impacted by variables such as heater eccentricity and Richardson number.

The relationship between the magnetic fields and heat transfer process, known as magnetohydrodynamics (MHD), adds another level of difficulty. Many researchers have investigated that magnetic fields may significantly affect the speeds at which heat is transferred and the fluid flow, which is relevant in a variety of applications from industry to biomedical engineering [11, 12]. The application of magnetic fields can be used to control heat transfer in MHD systems. Moreover, the existence of heat generation within cavities, whether from internal sources or external inputs, plays an important role in heat transfer processes. Temperature gradients and fluid flow patterns within the cavity can be affected by internal heat generation, which may result from a variety of sources, including chemical reactions, biological activities, and electrical waste.

2. Mathematical Formulations

2.1. Governing Equations

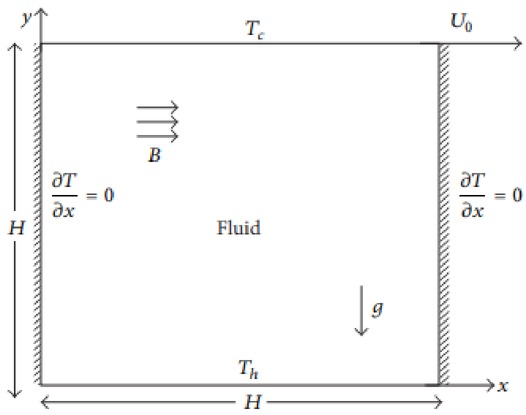

Figure 1: Geometrical configuration [13].

In Figure 1, a two-dimensional square cavity is shown. The value of length H represents the cavity's breadth and height. The bottom and top walls are not insulated, although both of the vertical walls are kept at two distinct yet constant temperatures, T_h and T_c, respectively, so that $T_h > T_c$. Moreover, it is assumed that the top lid travels in the positive direction of the *y*-axis at a constant speed, U_0. A horizontal magnetic field with a strength of B_0 is applied uniformly and normal to the adiabatic wall. When compared to the external magnetic field, the induced magnetic field caused by the velocity of the electrically conducting fluid is ignored. It is assumed that the working fluid is a laminar, unstable, incompressible, Newtonian flow. The downward gravitational force applies vertically. With the exception of the density, which fluctuates in accordance with the Boussinesq approximation in the body force term of the momentum equations, it is believed that the fluid's thermophysical parameters remain constant [13]. The fluid's temperature differential from the cold wall determines the uniform heat production or absorption that occurs in the cavity. While certain walls of the hollow are kept at constant temperatures T_h and T_c, where $T_h > T_c$, the lid of the cavity can move at a constant speed. Gravity is acting in the negative *y*-direction on the insulated sections of the remaining cavities [14]. From the above mentioned assumptions, the unsteady governing equations for conservations of mass, momentum, and energy can be written as follows;

Continuity Equation:

$$\frac{\partial u}{\partial x} + \frac{\partial v}{\partial y} = 0\,, \tag{2.1}$$

Momentum at *x*-axis:

$$u\frac{\partial u}{\partial x} + v\frac{\partial v}{\partial y} = -\frac{1}{\rho}\frac{\partial p}{\partial x} + v(\frac{\partial^2 u}{\partial x^2} + \frac{\partial^2 u}{\partial y^2})\,, \tag{2.2}$$

Momentum at *y*-axis:

$$u\frac{\partial u}{\partial x} + v\frac{\partial v}{\partial y} = -\frac{1}{\rho}\frac{\partial p}{\partial y} + v\left(\frac{\partial^2 v}{\partial x^2} + \frac{\partial^2 v}{\partial y^2}\right) + g\beta(T - T_c) - \frac{\sigma B^2}{\rho}v\,, \tag{2.3}$$

Energy Equation:

$$u\frac{\partial T}{\partial x} + v\frac{\partial T}{\partial y} = \alpha\left(\frac{\partial^2 T}{\partial x^2} + \frac{\partial^2 T}{\partial y^2}\right) + \frac{Q_0}{\rho_0 c_p}(T - T_c)\,. \tag{2.4}$$

where x and y are the Cartesian coordinate directions. The variable u, v, p, T, c_p are *x*-velocity, *y*-velocity, fluid pressure, fluid temperature, heat capacity respectively. The parameter $\beta, g, \sigma, v, \rho_0$ *and* Q_0 are fluid thermal expansion coefficient, gravity, fluid electrical conductivity, fluid kinematic viscosity, fluid density, and volumetric internal heat generation (Q_0 > 0), respectively. The parameter B_0 is the magnetic induction coefficient. The thermal diffusivity is defined as $\alpha = k/\rho c$, where *k* is the thermal conductivity and *c* is the heat capacity. The early stage boundary conditions of the problem are given as follows [13];

Top wall:	$u = U_0, \quad v = 0, \quad T = T_c\,,$	(2.5)
Bottom wall:	$u = v = 0, \quad T = T_h\,,$	(2.6)
Left and right walls:	$u = v = 0, \quad \frac{\partial T}{\partial x} = 0\,.$	(2.7)

Then, equations (2.1) to (2.4) are transformed to non-dimensional equations using the following variables:

$$X = \frac{x}{H}\,, \quad Y = \frac{y}{H}\,, \quad U = \frac{u}{U_0}\,, \quad V = \frac{v}{U_0}\,,$$

$$\theta = \frac{T - T_c}{T_h - T_c}\,, \quad Gr = \frac{g\beta(T - T_c)\,H^3}{v^2}\,, \quad Pr = \frac{v}{\alpha}\,, \quad P = \frac{p}{\rho U_0^2}\,,$$

$$Re = \frac{U_0 H}{v}\,, \quad Ha^2 = \frac{B_0^2 H^2 \sigma}{\rho v}\,, \quad \Delta = \frac{Q_0 L^2}{\rho_0 c_p \alpha}\,, \quad Ri = \frac{Gr}{Re^2}\,, \tag{2.8}$$

where θ and P is the non-dimensional temperature and the pressure, respectively. Parameters *Gr*, *Re*, *Pr*, Ha^2, Δ and Ri are the Grashof number, the Reynolds number, the Prandtl number, the Hartmann number, the heat generation or absorption parameter and the Richardson number respectively. Substituting the variables into the governing equations, we obtain the following non-dimensional equations:

Continuity Equation:

$$\frac{\partial U}{\partial X} + \frac{\partial V}{\partial Y} = 0\,, \tag{2.9}$$

Momentum at *x*-axis:

$$\boldsymbol{U}\frac{\partial \boldsymbol{U}}{\partial \boldsymbol{X}}+\boldsymbol{V}\frac{\partial \boldsymbol{V}}{\partial \boldsymbol{Y}}=-\frac{\partial \boldsymbol{P}}{\partial \boldsymbol{X}}+\frac{\boldsymbol{1}}{\boldsymbol{Re}}\left(\frac{\partial^2 \boldsymbol{U}}{\partial \boldsymbol{X}^2}+\frac{\partial^2 \boldsymbol{U}}{\partial \boldsymbol{Y}^2}\right), \tag{2.10}$$

Momentum at *y*-axis:

$$\boldsymbol{U}\frac{\partial \boldsymbol{U}}{\partial \boldsymbol{X}}+\boldsymbol{V}\frac{\partial \boldsymbol{V}}{\partial \boldsymbol{Y}}=-\frac{\partial \boldsymbol{P}}{\partial \boldsymbol{Y}}+\frac{\boldsymbol{1}}{\boldsymbol{Re}}\left(\frac{\partial^2 \boldsymbol{V}}{\partial \boldsymbol{X}^2}+\frac{\partial^2 \boldsymbol{V}}{\partial \boldsymbol{Y}^2}\right)+\frac{\boldsymbol{Gr}}{\boldsymbol{Re}^2}\boldsymbol{\theta}-\frac{\boldsymbol{Ha}^2}{\boldsymbol{Re}}\boldsymbol{V}, \tag{2.11}$$

Energy Equation:

$$\boldsymbol{U}\frac{\partial \boldsymbol{\theta}}{\partial \boldsymbol{X}}+\boldsymbol{V}\frac{\partial \boldsymbol{\theta}}{\partial \boldsymbol{Y}}=\frac{\boldsymbol{1}}{\boldsymbol{PrRe}}\left(\frac{\partial^2 \boldsymbol{\theta}}{\partial \boldsymbol{X}^2}+\frac{\partial^2 \boldsymbol{\theta}}{\partial \boldsymbol{Y}^2}\right)+\frac{\Delta}{\boldsymbol{PrRe}}\boldsymbol{\theta}. \tag{2.12}$$

The non-dimensional boundary conditions can be written as:

Top wall: $\boldsymbol{U}=\boldsymbol{1},\ \boldsymbol{V}=\boldsymbol{0},\ \boldsymbol{\theta}=\boldsymbol{0},$ (2.5)

Bottom wall: $U=V=0,\quad \theta=1,$ (2.6)

Left and right walls: $U=V=0,\quad \frac{\partial\theta}{\partial x}=0.$ (2.7)

3. Numerical Computation and Validation

3.1. Numerical Computation

Table 1: The average minimum velocity according to different types of meshes in COMSOL Multiphysics software.

Mesh	COMSOL Multiphysics mesh type	Average Min Velocity
Mesh 1	Normal	-0.28423
Mesh 2	Fine	-0.29376
Mesh 3	Finer	-0.30246
Mesh 4	Extra fine	-0.30695
Mesh 5	Extremely fine	-0.30739

To find the field variable grid-independency solutions, the grid sensitivity tests are conducted. The test is performed for *Ri* = 1.0, Pr = 6.2, and *Ha* = 60 in a top cooled moving lid, bottom heated, and vertically insulated cavity. The average min of velocity along the hot bottom wall are compared for the COMSOL Multiphysics mesh type from normal, fine, finer, extra fine and extremely fine.

3.2. Validation of Results

Table 2: Comparisons of the maximum and minimum values of the horizontal velocities in the mid-section of the cavity between the current solution and the proposed solution by [15] and [13].

	Re = 100.0		
	[15]	[13]	Present
$\boldsymbol{U_{min}}$	-0.2037	-0.2049	-0.2037
$\boldsymbol{U_{max}}$	1.0000	1.0000	1.000

To validate the findings that we detained using COMSOL Multiphysics software, the numerical results are compared to the previous published results as limiting cases. Table 2 shows a comparison between the current solutions and the previously published values [13, 15] for the maximum and minimum values of horizontal velocities at the mid-section of the cavity. The outcomes revealed a small difference between the numbers. This could be due to the slight variations of the software version between the older and latest versions of the COMSOL Multiphysics software.

4. Results and discussion

4.1. Velocity and Temperature Profiles

A numerical investigation is conducted on the mixed convection heat transfer in a lid-driven square cavity in the presence of heat generation and a magnetic field. The top and bottom vertical walls are maintained at distinct temperatures, and both are completely insulated. Water is used as the working fluid in the current analysis with Pr = 6.2. Hartmann number (*Ha*) and internal heat generation or absorption are the governing factors. The Reynolds number (*Re*=100) and the Grashof number ($Gr = 10^4$) are maintained constant. The magnetic field parameter values that were analysed were *Ha* = 0, 10, 30, and 60. Meanwhile, the internal heat generation or absorption parameter values that were collected were -5, 0, and 5. The heaters are located in the cavity's left-bottom corner. The obtained results are presented as streamlines and isotherms plottted under a mixed convection regime (*Ri* = 1.0).

4.1.1 The Effect of Magnetic Field

The streamlines and isotherms for different values of the Hartmann number (*Ha*) at Richardson number (*Ri*) = 1 are presented in Figure 4.1. The streamlines showed that most of the cavity is occupied by a clockwise recirculating vortex. This vortex's centre is close to the right wall, and streamlines that split apart around halfway through the cavity show that the sliding lid is primarily responsible for the shear-dominated fluid flow. When the magnetic field increases, the primary vortex takes on an increasingly circular form, while the spinning vortex loses intensity at *Ha* = 10. The core vortex is forced towards the top of the cavity when *Ha* increases to 30. The core vortex grows horizontally with increasing magnetic field intensity, suggesting a decrease in flow convection.

Streamline Isotherm

Ha = 0

Ha = 10

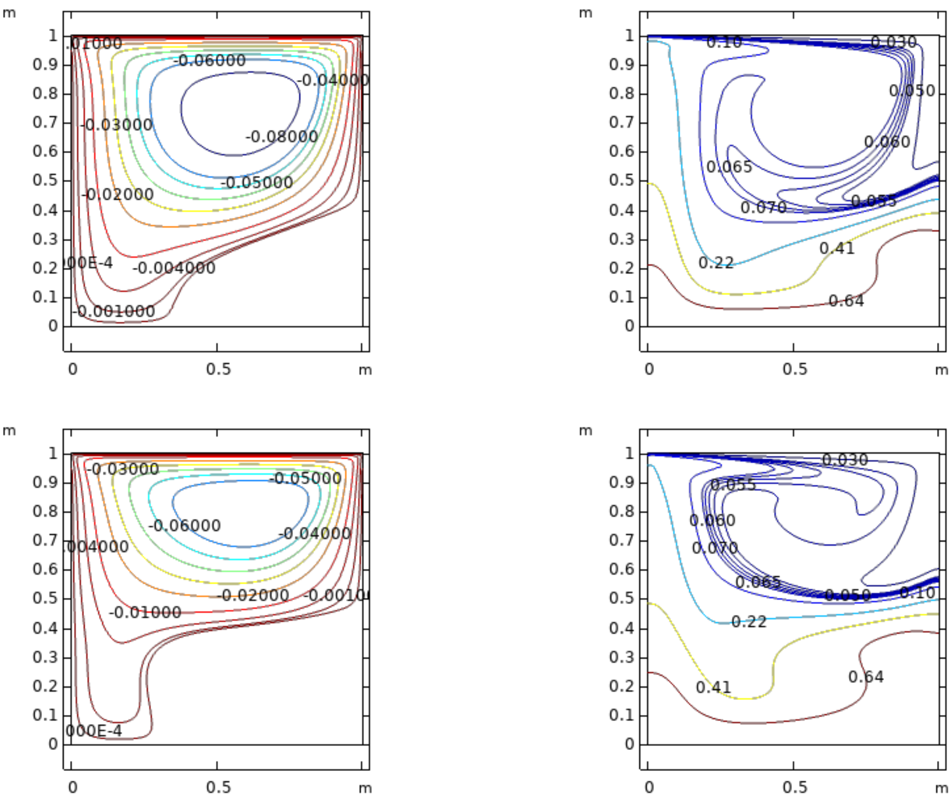

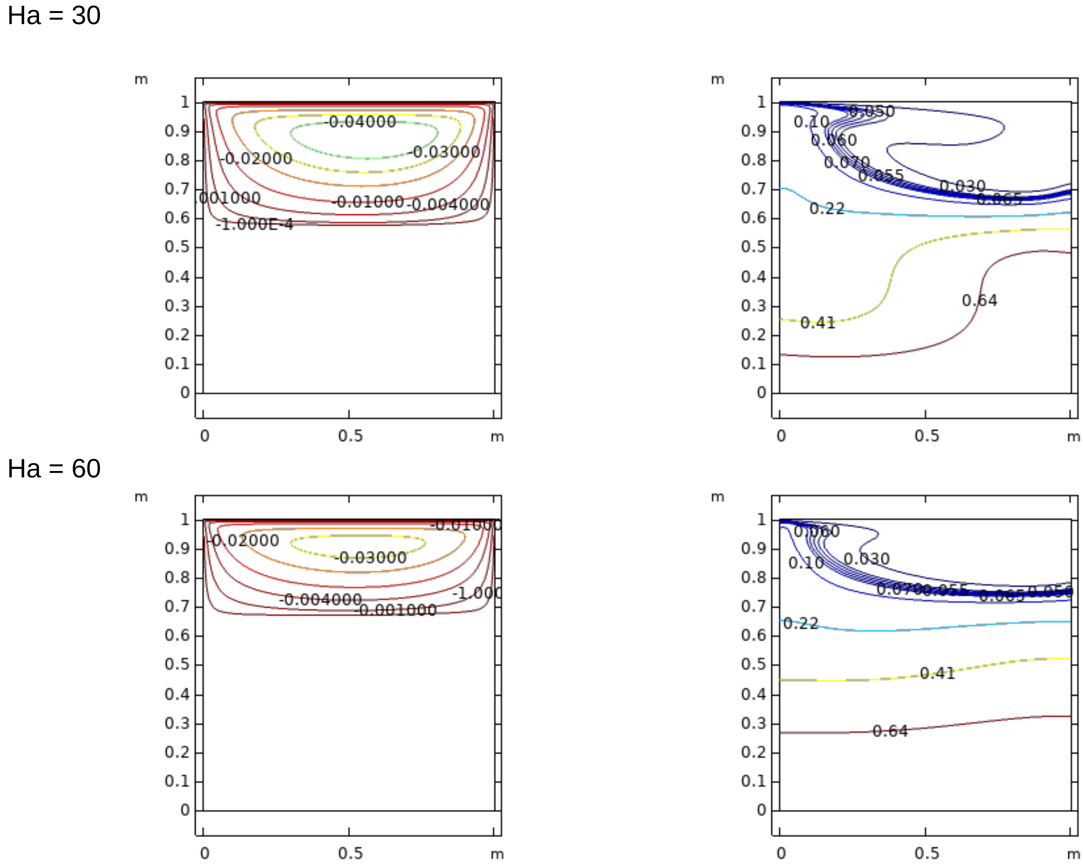

Figure 4.1 : Streamlines and isotherms with *Ri* = 1.0, *Gr* = 10^4, *Re* = 100, and different values of Hartmann Number.

Figure 4.1 demonstrated how *Ha* affects the isotherms. Because of the movement of the top wall, there is a strong temperature gradient close to the bottom right corner in the absence of a magnetic field. Temperature gradient, flow intensity, and velocity all decrease with increasing magnetic field strength. The isotherms are uniformly distributed close to the bottom wall and almost exactly parallel to the adiabatic wall. This suggests that the heat transmission becomes increasingly dominated by conductivity. The isotherms, which are uniformly distributed and are concentrated towards the cavity's bottom, demonstrate how the magnetic field inhibits the convective heat transfer process.

Overall, the findings showed that the flow dynamics and heat transfer properties in a lid-driven square cavity are greatly affected by raising the Hartmann number. Because of the sliding lid, the flow is mostly driven by shear forces at lower *Ha* values. A more stable, conduction-dominated temperature distribution is produced with higher *Ha* values when the magnetic field dampens the convective currents.

4.1.2 The Effect of Internal heat Generation or Absorption

Figure 4.2 illustrated the effect of internal heat generation or absorption on the streamlines and isotherms for a fixed Richardson number (*Ri* = 1.0). Both streamlines and isotherms displayed observable variations when internal heat generation or absorption occurs. A significant temperature gradient occured close to the heaters when internal heat absorption $\Delta = -5$ is enforced. The more noticeable thermal boundary layers in these areas provide as evidence for this. In contrast, the thermal boundary layers along the heaters weaken in the absence of internal heat generation or absorption. Strong thermal boundary layers occured along the cold wall when internal heat generation takes place, increasing the rate of heat transfer. When compared to the circumstances without internal heat generation Δ = 0, this makes the temperature gradients close to the heaters look smaller. Changes in internal heat generation or absorption characteristics have little effect on the fluid flow pattern itself. For *Ri* = 1.0, however, the stream function's absolute value increases in the presence of internal heat generation or absorption. The stream function's absolute value decreases with internal heat generation or absorption in the mixed convection dominated environment. On the other hand, the absolute value of the stream function increases with heat absorption in the buoyancy-dominated domain and decreases with a parameter value of Δ = 5.

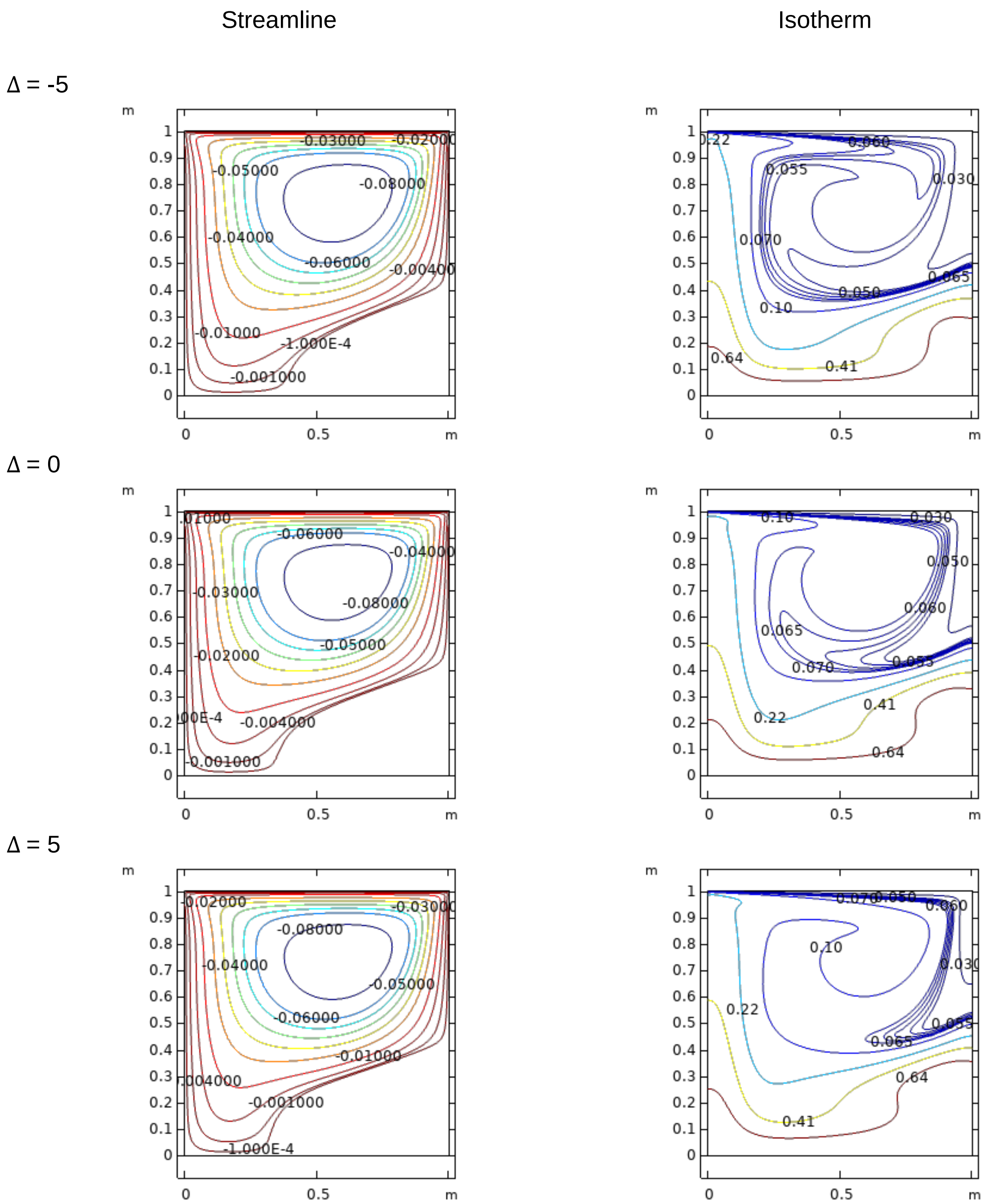

Figure 4.2 : Streamlines and isotherms with *Ri* =1.0, *Gr* = 10^4, *Re* = 100, and differernt values of Internal Heat Generation or Absorption.

Heat transfer rates and temperature distribution within the system are impacted by the overall thermal properties and flow dynamics that are mostly influenced by internal heat generation or absorption. To offer a more thorough knowledge of the phenomenon, future investigation might look into the potential interactions between changing the Richardson number and internal heat effects.

Conclusion

This study investigated the effects of magnetic field and heat generation on mixed convection in a lid-driven square cavity. The problem is modelled mathematically by the governing equations which include the continuity, momentum, and energy equations. The dimensional partial differential equations (PDEs) are transformed into non-dimensional PDEs by a similarity transformation. Then, using the finite element technique in the COMSOL Multiphysics software, these equations are numerically solved. The numerical results for the maximum and minimum values of the horizontal and vertical velocities at the mid-section of the cavity are compared with existing findings from published research in order to validate the precision of the algorithm developed in COMSOL Multiphysics software. Minor differences are observed, likely due to the use of different software versions. The study additionally examined on how various factors, such as the Grashof, Reynolds, Hartmann, and Richardson numbers, influence the streamlines and isotherm profiles. The important study results are analysed in detail as follow:

i. As the Hartmann number is increasing, the major recirculating eddy at the top wall to become larger and occupy the cavity.
ii. When the magnetic field is strenghtening, the flow strength is weakening.
iii. As the magnetic field strength is increase, the effect of convection is decreased.
iv. In the absence of internal heat generation or absorption, the thermal boundary layers near the heaters weaken.
v. Internal heat generation causes strong thermal boundary layers along the cold wall, increasing the rate of heat transfer.
vi. The tempreature gradients near the heaters appear smaller with internal heat generation compared to without it.
vii. The overall fluid flow pattern remains largely unaffected by internal heat generation or absorption.
viii. However, the absolute value of the stream function increases with internal heat generation or absorption at Ri = 1.0.

Acknowledgement

The author would like to thank everyone who helped to complete this research with the deepest thanks and appreciation.

References

[1] A. R. M. Rosdzimin, S. M. Zuhairi, & C. S. N. Azwadi. (2022). Simulation of Mixed Convective Heat Transfer using Lattice Boltzmann Method. *International Journal of Automotive and Mechanical Engineering*, *2*, 130–143. Retrieved from https://journal.ump.edu.my/ijame/article/view/8044

[2] Koseff, J. R., & Street, R. L. (1984). On end wall effects in a LID-Driven cavity flow. *Journal of Fluids Engineering-transactions of the Asme*, *106*(4), 385–389. https://doi.org/10.1115/1.3243135.

[3] Prasad, A. K., & Koseff, J. R. (1989). Reynolds number and end-wall effects on a lid-driven cavity flow. *Physics of Fluids*, *1*(2), 208–218. https://doi.org/10.1063/1.857491.

[4] Ghia, U., Ghia, K., & Shin, C. (1982). High-Re solutions for incompressible flow using the Navier-Stokes equations and a multigrid method. *Journal of Computational Physics*, *48*(3), 387-411. https://doi.org/10.1016/0021-9991(82)90058-4.

[5] Perumal, D. A., Kumar, G. V., & Dass, A. K. (2012). Numerical Simulation of Viscous Flow over a Square Cylinder Using Lattice Boltzmann Method. *ISRN Mathematical Analysis (Print)*, *2012*, 1–16. https://doi.org/10.5402/2012/630801.

[6] Gibanov, N. S., Sheremet, M. A., Oztop, H. F., & Al-Salem, K. (2017). Convective heat transfer in a lid-driven cavity with a heat-conducting solid backward step under the effect of buoyancy force. *International Journal of Heat and Mass Transfer*, *112*, 158-168. https://doi.org/10.1016/j.ijheatmasstransfer.2017.04.102.

[7] Bhopalam, S. R., Perumal, D. A., & Yadav, A. K. (2021). Computational appraisal of fluid flow behavior in two-sided oscillating lid-driven cavities. *International Journal of Mechanical Sciences*, *196*, 106303. https://doi.org/10.1016/j.ijmecsci.2021.106303.

[8] Merkin, J. H., Pop, I., Lok, Y. Y., & Groşan, T. (2022). Nanofluids. *Similarity Solutions for the Boundary Layer Flow and Heat Transfer of Viscous Fluids, Nanofluids, Porous Media, and Micropolar Fluids*, 87–112. https://doi.org/10.1016/b978-0-12-821188-5.00005-9

[9] Oztop, H. F., & Dagtekin, I. (2004). Mixed convection in two-sided lid-driven differentially heated square cavity. *International Journal of Heat and Mass Transfer*, *47*(8-9), 1761- 1769. https://doi.org/10.1016/j.ijheatmasstransfer.2003.10.016.

[10] Islam, A. W., Sharif, M. A., & Carlson, E. S. (2012). Mixed convection in a lid driven square cavity with an isothermally heated square blockage inside. *International Journal of Heat and Mass Transfer*, *55*(19-20), 5244-5255. https://doi.org/10.1016/j.ijheatmasstransfer.2012.05.032

[11] Sivasankaran, S., Malleswaran, A., Lee, J., & Sundar, P. (2011). Hydro-magnetic combined convection in a lid-driven cavity with sinusoidal boundary conditions on both sidewalls. *International Journal of Heat and Mass Transfer*, *54*(1–3), 512–525. https://doi.org/10.1016/j.ijheatmasstransfer.2010.09.018.

[12] Farahani, S. D., Amiri, M., Majd, B. K., & Mosavi, A. (2021). Effect of magnetic field on heat transfer from a channel: Nanofluid flow and porous layer arrangement. *Case Studies in Thermal Engineering*, *28*, 101675. https://doi.org/10.1016/j.csite.2021.101675.

[13] Bakar, N. A., Karimipour, A., & Roslan, R. (2016). Effect of magnetic field on mixed convection heat transfer in a LID-Driven square cavity. Journal of Thermodynamics, 2016, 1–14. https://doi.org/10.1155/2016/3487182.

[14] Sivasankaran, S., Sivakumar, V., Hussein, A. K., & Prakash, P. (2013). Mixed Convection in a Lid-Driven Two-Dimensional Square Cavity with Corner Heating and Internal Heat Generation. *Numerical Heat Transfer Part A-applications*, *65*(3), 269–286. https://doi.org/10.1080/10407782.2013.826017.

[15] Khanafer, K. M., & Chamkha, A. J. (1999). Mixed convection flow in a lid-driven enclosure filled with a fluid-saturated porous medium. *International Journal of Heat and Mass Transfer/International Journal of Heat and Mass Transfer*, *42*(13), 2465–2481. https://doi.org/10.1016/s0017-9310(98)00227-0.